UCRL-JRNL-217376

Study of f electron correlations in nonmagnetic Ce by means of spin resolved resonant photoemission

S.-W. Yu, T. Komesu, B. W. Chung, G. D. Waddill, S. A. Morton, J. G. Tobin

November 30, 2005

Disclaimer

This document was prepared as an account of work sponsored by an agency of the United States Government. Neither the United States Government nor the University of California nor any of their employees, makes any warranty, express or implied, or assumes any legal liability or responsibility for the accuracy, completeness, or usefulness of any information, apparatus, product, or process disclosed, or represents that its use would not infringe privately owned rights. Reference herein to any specific commercial product, process, or service by trade name, trademark, manufacturer, or otherwise, does not necessarily constitute or imply its endorsement, recommendation, or favoring by the United States Government or the University of California. The views and opinions of authors expressed herein do not necessarily state or reflect those of the United States Government or the University of California, and shall not be used for advertising or product endorsement purposes.

Study of f electron correlations in nonmagnetic Ce by means of spin resolved resonant photoemission

S.-W. Yu,[1] T. Komesu,[2] B. W. Chung,[1] G. D. Waddill,[2] S. A. Morton,[1,2] and J. G. Tobin[1]

[1]*Lawrence Livermore National Laboratory, Livermore, California 94550, USA*

[2]*Physics Department, University of Missouri-Rolla, Rolla, Missouri 65409, USA*

Abstract

We have studied the spin-spin coupling between two f electrons of nonmagnetic Ce by means of spin resolved resonant photoemission using circularly polarized synchrotron radiation. The two f electrons participating in the $3d_{5/2} \rightarrow 4f$ resonance process are coupled in a singlet while the coupling is veiled in the $3d_{3/2} \rightarrow 4f$ process due to an additional Coster-Kronig decay channel. The identical singlet coupling is observed in the $4d \rightarrow 4f$ resonance process. Based on the Ce measurements, it is argued that spin resolved resonant photoemission is a unique approach to study the correlation effects, particularly in the form of spin, in the rare-earths and the actinides.

In photoemission investigations of nonmagnetic materials, the measurement of electron spin polarization with respect to a suitably chosen quantization direction can provide new insight into the electronic structure of the systems under study, beyond that which can be gleaned from merely the energy and momentum relationship of the photoelectrons [1, 2]. For example, the spin polarized photoemission experiment performed with circularly polarized light, in which spin polarization is aligned with photon propagation direction, is an essential method to characterize the symmetries of the states. These measurements permit the performance of the symmetry resolved band mapping of solids [3, 4] and the determination of all dipole matrix elements and phase-shift differences of continuum wave functions describing the photoelectron emission from free and absorbed atoms [5]. The combination of a spin-orbit interaction and circularly polarized light induces an anisotropic distribution of the m_j in the final state wave function via the relativistic dipole selection rules. To a great extent, these measurements are extensions of the Fano effect, first predicted [6] and observed [7] over 30 years ago.

The photoexcitation of core electrons by circularly polarized light in nonmagnetic materials will not only result in the spin polarization of the ejected photoelectrons [8] but also in spin polarized core holes aligned with photon spin. These spin polarized core holes can decay by emission of polarized photons or by spin dependent Auger processes [9–16]. For example, consider the CVV (core valence valence) Auger process in a solid. The initial state is two valence electrons and final state is two electron states in which one of them has filled the polarized hole and another one is ejected as an Auger electron. If the two valence electrons are coupled in a singlet, the spin of the outgoing electron has to be antiparallel to the spin of the primary core hole, due to the selection rules governing Auger process ($\Delta S = 0$) [17]. If the two valence electrons are coupled in a triplet, the spin of the outgoing electron has to be parallel to the spin of the primary core hole. Therefore, the spin analysis of the photoelectrons and the corresponding Auger electrons allows the study of the spin-spin coupling between the two valence electrons participated in the CVV decay process from the nonmagnetic materials.

In the above context, this paper reports on the spin resolved measurements of the $3d \rightarrow 4f$ resonant photoemission in nonmagnetic Ce, as a means of studying electron correlations between f electrons. Furthermore, because Ce is the first element of the rare-earths and the location of the delocalized/localized transition in the rare earths [18], the results from

Ce may serve as a prototype for the other rare-earths and the actinides as well, in which strong correlation effects originating from highly localized f electrons may play the crucial role for the determination of the physical properties [19–22]. Here, it will be shown that spin resolved resonant photoemission spectroscopy, using circularly polarized light, can provide a direct means of investigating electron correlation in nonmagnetic materials. In this case, it will be shown that electron-electron coupling in the Auger-like decay process can be observed in a unique and powerful manner.

The experiments were performed at beamline 4-ID-C of the Advanced Photon Source, Argonne National Laboratory [23]. The beamline provides circularly polarized x-rays, with switchable helicities ($\sigma^{\pm}$) on demand, with a degree of polarization $>96\%$ in the energy range of $500-3000$ eV. The total resolution (beamline + analyzer) of 0.8 eV was chosen to allow a reasonable signal in the Mott detector, since the efficiency of the Mott detector ($S^2 I/I_0$) is of order 10^{-5}. The experimental apparatus used in the present study has been previously described [24–26]. Uncrystallized cerium samples were made by evaporation *in situ* on a W(110) substrate at room temperature [27]. The base pressures were in the low 10^{-11} torr range, rising to $\sim 6\times10^{-10}$ torr during evaporation. The cleanliness of the Ce samples was monitored by O $1s$ signal. Photon energies were calibrated using the $3d_{5/2} \rightarrow 4f$ transition in x-ray absorption spectroscopy (XAS), at energy of 882.2 eV [28].

For our purposes the $3d \rightarrow 4f$ transition of Ce is an excellent choice because the spin-orbit split $3d_{5/2}$ and $3d_{3/2}$ levels are well separated by 18.5 eV in binding energy [19]. Thus well defined and oppositely spin polarized core holes can potentially be generated by photoexcitation using circularly polarized light into $4f$ final states. The $3d \rightarrow 4f$ resonance arises when an interference occurs between the direct photoemission channel

$$3d^{10}4f^1 + h\nu \rightarrow 3d^{10}4f^0 + \text{electron} \tag{1}$$

and indirect channel in which there is the $3d \rightarrow 4f$ excitation with subsequent CVV Auger-like decay

$$3d^{10}4f^1 + h\nu \rightarrow 3d^9 4f^2 \rightarrow 3d^{10}4f^0 + \text{electron} \tag{2}$$

which has the identical initial and final state with the direct channel. Since the condition for the interference is coherence between the direct and the indirect channels, the loss of coherence can be due either to delocalization of the $4f$ electrons in the intermediate state, which produce an energy difference between the final states of the two channels or to a

different time for the two channels [29, 30]. Therefore, the sharp resonance in the $3d \rightarrow 4f$ transition is consistent with the strongly localized nature of $4f$ wave functions in rare earths [28].

A spin resolved core level spectrum is shown in Fig. 1. Here, the Ce $3d_{5/2}$ level at a binding energy of 883.8 eV is undergoing interrogation with photons of 1375 eV. This core level will be one of those used in the resonant photoemission study. Measurements of its spin polarization is essential to establishing the initial polarizations of the core holes and testing the validity of our relativistic models. In order to eliminate the instrumental asymmetry, the electron spin polarization P_Z aligned to photon spin is determined from the raw spectra using the following formula

$$P_Z = \frac{1}{S \cdot P_\sigma \cdot \cos 55} \cdot \left(\frac{\sqrt{N_1^+ N_3^-} - \sqrt{N_1^- N_3^+}}{\sqrt{N_1^+ N_3^-} + \sqrt{N_1^- N_3^+}} \right). \tag{3}$$

Here, $N_{1(3)}^\pm$ is the intensity with $\sigma^\pm$ at the counters 1(3) located at equal polar angles 120° in the reaction plane defined by incoming and scattered electron beam, S is Sherman function, P_σ is light polarization, and $\cos 55°$ is due to the 55° off-normal incidence of light and normal emission of electrons. It should be noted that the instrumental asymmetry A_Z defined in the following way

$$A_Z = \frac{\sqrt{N_1^+ N_1^-}}{\sqrt{N_3^+ N_3^-}} \tag{4}$$

has to be monitored for every run to determine the electron spin polarization correctly [31]. If A_Z differs from 1, this means that there is an instrumental asymmetry. The instrumental asymmetry can be eliminated by using the equation (3) only if A_Z does not vary in time [31]. Therefore, monitoring of A_Z provides an important check on the performance of the Mott detector. If A_Z is not constant over runs, the spin polarization determined by using equation (3) cannot be claimed to be accurate. For example, the bottom panel of Fig. 1 shows that we have an instrumental asymmetry because A_Z differs from 1, and that the instrumental asymmetry can be eliminated by using equation (3) because A_Z is constant over runs. The middle panel of Fig. 1 shows the P_Z measured by using equation (3).

In the top of Fig. 1, the spin separated partial intensities I_+ and I_- are connected with the measured spin polarization P_Z and the measured total (spin independent) intensity I by $I_\pm = I/2(1 \pm P_Z)$. Correspondingly, I_+ and I_- are the partial intensities polarized totally parallel and antiparallel to the photon spin, respectively. From the total intensity I, a strong

main peak A centered at a binding energy of 883.8 eV and a weak peak B centered at a binding energy of ~ 878 eV are visible. The physical origin of the two peaks is as follows. Because $4f$ states are localized in the $3d$ core region, they are extremely sensitive to the attractive Coulomb potential of the $3d$ hole. Consequently, the creation of a $3d$ core hole by photoexcitation causes an additional empty $4f$ state to be pulled down below the Fermi energy. Thus, in a very simple picture, two final states are produced: when the empty $4f$ state is not yet occupied and the screening is produced by the $(5d6s)^3$ valence band, the result is a final state with a configuration of $3d^9 4f^1$ (peak A). If the empty $4f$ state is filled by an extra f electron from the conduction band and it screens the core hole, this is another final state with a configuration of $3d^9 4f^2$ (peak B). The second final state with the configuration of $3d^9 4f^2$ has much weaker intensity and smaller binding energy [19, 32, 33]. From the spin separated partial intensities I_+ and I_-, it can be seen that I_+ is dominant over peak A, with an approximately $+20\%$ spin polarization. It is interesting to note that the peak B is also slightly positively polarized.

We use the three step model of photoemission in the interpretation of the spin resolved spectra, which is consists of (i) the primary excitation process in the bulk by absorption of the incident photon, (ii) the transport of the excited electron to the surface which includes the possibility for inelastic scattering by the electron-electron and the electron-phonon, and (iii) the escape of the electron through the surface into the vacuum [34]. In principal, every one of these three steps may result in a nonzero contribution to the net spin polarization. For centrosymmetric nonmagnetic materials with no preferential population of one spin state in the ground state, however, it is demonstrated that the first step, the primary excitation process, is main responsible for nonzero spin polarization if the exciting light is circularly polarized [2]. The second step, transport to the surface, produces no net spin polarization in nonmagnetic materials [2]. In the third step, off-normally emitted photoelectrons may require a nonzero contribution to the net spin polarization during their transmission through the surface due to the spin-dependent diffraction of the photoelectrons at the surface [35–37]. However, this contribution to the net spin polarization vanishes for the symmetry reasons for normal emission to the surface [35]. Therefore, nonmagnetic materials and normal emission of electrons ensure that the second and the third step of the three step model of photoemission are spin independent, and the spin polarization is dominated by the primary excitation known as optical spin orientation [1, 2]. Fig. 2 illustrates a scheme of optical spin

orientation in an atom for the $d \to f$ transition with σ^+. Positive and negative numbers in the rectangles represent the angle integrated spin polarizations for given m_j using Clebsch-Gordan coefficients. The arrows indicate the allowed transitions between initial and final states via relativistic dipole selection rules for σ^+ with the transitions probabilities calculated using the spherical harmonics with the assumption of identical radial parts of the $d_{5/2}$- and $d_{3/2}$-wave functions in the initial states and of the $f_{7/2}$- and $f_{5/2}$-wave functions in the final states. Because the spin polarization of the final states lead to spin resolved photoemission if their energy lie above the vacuum level, the spin polarization of photoelectrons can be calculated using the following expression

$$ P = \frac{\sum\limits_{i=-J}^{J} a_i s_i}{\sum\limits_{i=-J}^{J} a_i}. \tag{5} $$

Here, a_i is the transition probabilities and s_i is the spin polarizations of the final states. Using equation (5) and Fig. 2, the transitions $d_{5/2} \to f(f_{7/2}+f_{5/2})$ and $d_{3/2} \to f_{5/2}$ result in the spin polarizations of $+60\%$ and -50%, respectively. It should be noted that the $d_{5/2} \to f_{5/2}$ transition gives a negative spin polarization, but it has 20 times weaker transition probability than that of the $d_{5/2} \to f_{7/2}$. Therefore, $d_{5/2} \to f$ $(f_{7/2}+f_{5/2})$ transition gives a net positive spin polarization of photoelectrons.

We notice that there is a poor agreement between the measured spin polarization of $+20\%$ and the calculated one of $+60\%$ for $d_{5/2} \to f(f_{7/2}+f_{5/2})$ transition. For this discrepancy, we should note the following two points. Firstly, the measured partial intensities I_+ and I_- include the unpolarized background. A proper subtraction of the background from the partial intensities I_+ and I_- results in a spin polarization of approximately $+44\%$ in the peak A which is much closer to $+60\%$. Secondly, the atomic model used in Fig. 2 oversimplifies the real system. For example, the spin polarization of $3d_{5/2} \to 4f$ transition depends on photon energy through the radial parts of the matrix elements [6, 8], but the dependency is not included in the atomic model. In any cases, even though the atomic model given in Fig. 2 describes the system under study qualitatively only, it is extremely useful because it presents a simple picture how photoelectrons are spin polarized without any complicated calculations.

Another aspect of the spin resolved direct photoemission of core levels is that it provides an important illustration of generation of a spin polarized core hole, which is the basic

6

source for nonzero spin polarization in the resonant photoemission experiment. In the direct photoemission of core levels, the circularly polarized light produces spin polarized photoelectrons due to the relativistic dipole selection rules. This means, because photoelectrons are spin polarized, they should leave behind spin polarized core holes in the initial states. Based on Fig. 2, due to the different transition probabilities for the different m_j, the $3d_{5/2}$ $\rightarrow 4f$ transitions with σ^+ give rise to an anisotropic excitation in the m_j of $3d_{5/2}$, generating a net $+47\%$ spin polarized core hole in the $3d_{5/2}$ state. Here, equation (5) has been used by substituting s_i with the spin polarizations of m_j of $3d_{5/2}$ state. The meaning of spin polarized core hole is that the sum of the m_j of $3d_{5/2}$ core holes is not equal to zero [9]. In the same way, the $3d_{3/2} \rightarrow 4f$ transitions create a -30% spin polarized core hole in the $3d_{3/2}$ state. These spin polarized core holes will decay by spin-dependent CVV Auger processes, contributing to the resonant photoemission through the indirect channel.

Now, let us consider the resonant photoemission itself. Fig. 3 (b) and (c) present spin resolved resonant photoemission measured at the $3d_{5/2} \rightarrow 4f$ transition at hν = 882.2 eV and the $3d_{3/2} \rightarrow 4f$ transition at hν = 899.4 eV. At the $3d_{5/2} \rightarrow 4f$ resonance, the partial intensity I_- is dominant over the two peaks labelled as f^0 and f^1 [19, 38], with a monotonic -20% spin polarization. This observation and the impact of the negative spin polarization at the $3d_{5/2} \rightarrow 4f$ resonance is the main message of this paper. As sketched at the (a) of Fig. 4, we propose a simplified physical explanation for the measured spin polarization. The positively spin polarized core holes in the $3d_{5/2}$ state decay obeying the selection rule for the CVV Auger-like process; the two valence f electrons coupled in a singlet participate in the decay process, resulting in -20% spin polarization. In principal, the spin polarization from the direct photoemission and the indirect CVV part can both contribute to the spin polarization measured at resonance. As shown below, however, the contribution from the direct photoemission can be suppressed because the uncrystallized Ce samples instead of a single crystal were used in the measurements. In photoemission from nonmagnetic valence bands, a significant nonzero spin polarization can be expected only at points and along lines of high symmetry in the Brillouin zone because there are the spatially degenerated bands and spin-orbit interaction splits the bands. These bands modified by spin-orbit interaction and circularly polarized light are the necessary conditions for nonzero spin polarization. However, at the general points of Brillouin zone, where there are no spatially degenerated bands to be modified by spin-orbit interaction, photoelectrons are unpolarized giving equal amounts of

7

'up' and 'down' spins [1, 39]. An example is the spin resolved valence band photoemission from Ge: electrons emitted from Ge(001) single crystal using circularly polarized light are highly spin polarized while electrons emitted from amorphous Ge film at the same photon energy are unpolarized [1]. Since we used uncrystallized Ce samples, which has no well defined points and lines of symmetry, we expect that there is no contribution in the measured spin polarization from the direct photoemission. Therefore, it is concluded that the -20% spin polarization measured in the resonant spectra results from correlations in the spins between the polarized core holes and the outgoing Auger electrons, mediated by two valence f electrons coupled in a singlet.

The appearance of the two peaks f^0 and f^1 is a characteristic of the highly localized nature of $4f$ electrons assumed to be similarly localized to core electrons. A hole created in the $4f$ state by photoemission acts as an additional attractive potential for the other electrons in the system, generating complicated final states as f^0 and f^1 [19]. The monotonic spin polarization measured over the two peaks f^0 and f^1 indicates that the f^0 and f^1 states are resonated with the identical spin structure. It should be noted that the two peaks f^0 and f^1 are also assigned as the lower Hubbard band and the quasiparticle peak, respectively [40–42].

In the same vein, a positive spin polarization is expected at the $3d_{3/2} \rightarrow 4f$ resonance because of a negatively spin polarized core hole in the $3d_{3/2}$ state. As shown in Fig. 3 (c), however, no spin polarization is observed at the $3d_{3/2} \rightarrow 4f$ resonance, within the statistics. In addition, a direct comparison of the total intensities of the $3d_{5/2} \rightarrow 4f$ and the $3d_{3/2} \rightarrow 4f$ transitions at the position of f^0, indicates that there is an approximately 6.5 times reduction in the intensity at the $3d_{3/2} \rightarrow 4f$ resonance relative to that at the $3d_{5/2} \rightarrow 4f$ resonance. It appears that CVV indirect channel of the $3d_{3/2}$ core hole has been quenched by a new competitive decay channel, a Coster-Kronig(CK) transition where the spin polarized core hole in $3d_{3/2}$ state is filled by electrons from the $3d_{5/2}$ state, resulting in spin polarized holes in $3d_{5/2}$ and the production of off-resonance electrons with lower kinetic energy. Since the CK transition commonly occurs with 1-3 orders of magnitude greater probability than usual Auger decay and degrades the spin polarization of the polarized holes in the $3d_{3/2}$ [9, 43], the consequence is the substantial decrease of the intensity and the spin polarization at the $3d_{3/2} \rightarrow 4f$ resonance. A sketch for that is given in the (b) of Fig. 4.

The comparison between the -20% spin polarization measured at the $3d_{5/2} \rightarrow 4f$ resonance and the -47% spin polarization of the $3d_{5/2}$ core holes calculated using atomic model

shows clearly a considerable discrepancy, although we understand that the atomic model explains the measured spin polarization qualitatively only. Even though the discrepancy does not prevent us from the understanding of the spin-spin coupling basically, some possible reasons for the discrepancy are addressed in the following.

(1) Triplet coupled two electrons may participate in the resonant process. Although the singlet coupling is favored, triplet coupling may have some influence.

(2) A recent publication on Ce compounds [44] indicated that there are incoherent Auger transition between different multiplet states of $3d^9 4f^2$ configuration in the resonant process. Assuming the incoherent Auger electrons are unpolarized, they are overlapped with the main resonant signal as unpolarized background, and thereby lowering the spin polarization [45].

(3) Because the matrix element of the Auger process is described by the integration of the initial state (two $4f$ states representing two f electrons) and the final state ($3d$ core state and a continuum wave function representing the Auger electron), the overlap of the wave functions of the initial and the final states may play a role for an effective correlation between electrons involved in the Auger process. A complete overlap between those wave functions could result in a large exchange interaction, causing a complete spin correlation of electrons involved in the Auger process, while a relatively small overlap could result in a small correlation, reducing the spin polarization of the Auger electron. In fact, the overlap between $4d$ and $4f$ wave functions is stronger than that between $3d$ and $4f$ wave functions [28]. In support of the above argument, spin resolved resonance spectra of the $4d \rightarrow 4f$ resonance at hν=127 eV using circularly polarized light are shown in Fig. 5. The measurements with the uncrystallized Ce sample were performed at the Beamline 4 at the Advanced Light Source, Lawrence Berkeley National Laboratory and a detailed experimental setup is described elsewhere [46]. At the $4d$ threshold, both pre-edge structure and a broad giant resonance, which are manifestation of strong Coulomb and exchange interaction between $4d$ and $4f$ [18, 30], are observed in the x-ray absorption spectroscopy as shown in the (a) of Fig. 5. The (b) and (c) of Fig. 5 illustrate spin resolved resonant photoemission spectra measured at hν=127 eV along Z-direction aligned with photon propagation direction and along X-direction perpendicular to that, respectively. It is clear that because the incoming circularly polarized light creates spin polarized core holes aligned with photon propagation direction, there is no physical driving force for nonzero spin polarization along X-direction. As shown in the (c) of Fig. 5, P_X is equal to zero within the statistic error bars. The

physical origin of the measured spin polarization P_Z at the $4d \rightarrow 4f$ resonance is also the spin polarized core holes at the $4d_{5/2}$ created by circularly polarized light. The spin-orbit coupling of $4d_{5/2}$ and $4d_{3/2}$ is small. However, the core holes generated at the $4d_{3/2}$ edge decay via the CK transition into the $4d_{5/2}$ core holes. Therefore, the $4d_{3/2}$ core holes do not influence the spin polarization measured at the $4d \rightarrow 4f$ resonance [9]. From the (b) of Fig. 5, spin polarization P_Z measured over the $4d \rightarrow 4f$ resonance is approximately -43%, which agrees almost quantitatively with the -47% predicted by atomic model. Thus "overlap" scenario may explain why the spin polarization measured at the $3d_{5/2} \rightarrow 4f$ resonance is low. A detailed analysis of spin-resolved resonance spectra at the $4d \rightarrow 4f$ resonance will be published in a separate publication.

In conclusion, spin dependent resonant photoemission using circularly polarized light has been applied to explore the spin-spin coupling between two f electrons of strongly correlated nonmagnetic Ce. Positively and negatively spin polarized core holes are created at spin-orbit split $3d_{5/2}$ and $3d_{3/2}$ states, respectively, by direct photoemission using circularly polarized light. At the $3d_{5/2} \rightarrow 4f$ resonance, the measured monotonic negative spin polarization reveals a dominant singlet coupling between two $4f$ electrons participating in the resonant process. Because the Auger process is driven by a Coulomb interaction, the singlet coupling is favored because it allows the two electrons to be in greater proximity than the triplet coupling. At the $3d_{3/2} \rightarrow 4f$ resonance the spin polarization is quenched via an additional CK process. The negative spin polarization measured at the $4d \rightarrow 4f$ resonance also supports the singlet coupling. Based on the Ce results, we would like to suggest that spin dependent resonant photoemission may provide an excellent way to probe the f electron correlations in the rare-earths and the actinides. Finally, from the experimental point of view, theoretical calculations for spin resolved resonant photoemission are highly desirable to understand the electron correlations quantitatively.

Department of Energy.

[1] F. Meier and D. Pescia, *Optical Orientation* edited by F. Meier and B. P. Zakharchenya (Elsevier, Amsterdam, 1984).

[2] M. Wöhlecke and G. Borstel, *Optical Orientation* edited by F. Meier and B. P. Zakharchenya (Elsevier, Amsterdam, 1984).

[3] B. Kessler, A. Eyers, K. Horn, N. Müller, B. Schmiedeskamp, G. Schönhense, and U. Heinzmann, Phys. Rev. Lett. **59**, 331 (1987).

[4] S.-W. Yu, N. Müller, U. Heinzmann, C. Pettenkofer, A. Klein, and P. Blaha, Phys. Rev. B **69**, 045320 (2004).

[5] U. Heinzmann, Phys. Scr. **T17**, 77 (1987).

[6] U. Fano, Phys. Rev. **178**, 131(1969); **184**, 250 (1969).

[7] U. Heinzmann, J. Kessler, and J. Lorenz, Phys. Rev. Lett. **25**, 1325 (1970).

[8] K. Starke, A. P. Kaduwela, Y. Liu, P. D. Johnson, M. A. Van Hove, C. S. Fadley, V. Chakarian, E. E. Chaban, G. Meigs, and C. T. Chen, Phys. Rev. B **53**, R10544 (1996).

[9] P. Stoppmanns, Ph.D. thesis, Universität Bielefeld, Germany, 1995.

[10] R. David, M. Scheuer, P. Stoppmanns, S.-W. Yu, N. Müller, and U. Heinzmann, J. Electron Spectrosc. Relat. Phenom **93**, 153 (1998).

[11] N. Müller, T. Lischke, M. R. Weiss, and U. Heinzmann, J. Electron Spectrosc. Relat. Phenom **114-116**, 777 (2001).

[12] G. Snell, B. Langer, M. Drescher, N. Müller, B. Zimmermann, U. Hergenhahn, J. Viefhaus, U. Heinzmann, and U. Becker, Phys. Rev. Lett. **82**, 2480 (1999).

[13] T. Kachel, R. Rochow, W. Gudat, R. Jungblut, O. Rader, and C. Carbone, Phys. Rev. B **45**, 7267 (1992).

[14] L. H. Tjeng, B. Sinkovic, N. B. Brookes, J. B. Goedkoop, R. Hesper, E. Pellegrin, F. M. F. de Groot, S. Altieri, S. L. Hulbert, E. Shekel, and G. A. Sawatzky, Phys. Rev. Lett. **78**, 1126 (1997).

[15] N. B. Brookes, G. Ghiringhelli, O. Tjernberg, L. H. Tjeng, T. Mizokawa, T. W. Li, and A. A. Menovsky, Phys. Rev. Lett. **87**, 237003 (2001).

[16] P. G. Steeneken, L. H. Tjeng, I. Elfimov, G. A. Sawatzky, G. Ghiringhelli, N. B. Brookes, and

D.-J. Huang, Phys. Rev. Lett. **88**, 47201 (2002).

[17] T. A. Carlson, *Photoelectron and Auger Spectroscopy* (Plenum Press, New York. 1975).

[18] K. T. Moore, B. W. Chung, S. A. Morton, A. J. Schwartz, J. G. Tobin, S. Lazar, F. D. Tichelaar, H. W. Zandbergen, P. Söderlind, and G. van der Laan, Phys. Rev. B **69**, 193104 (2004).

[19] S. Hüfner, *Photoelectron Spectroscopy, 3th Edition* (Springer-Verlag, Berlin, 2003).

[20] R. C. Albers, Nature **410**, 759 (2001).

[21] S. Y. Savrasov, G. Kotliar, and E. Abrahams, Nature **410**, 793 (2001).

[22] J. G. Tobin, K. T. Moore, B. W. Chung, M. A. Wall, A. J. Schwartz, G. van der Laan, and A. L. Kutepov, Phys. Rev. B **72**, 085109 (2005).

[23] J. W. Freeland, J. C. Lang, G. Srajer, R. Winarski, D. Shu, and D. M. Mills, Rev. Sci. Instrum. **73**, 1408 (2002).

[24] M. Hochstrasser, J. G. Tobin, E. Rotenberg, and S. D. Kevan, Phys. Rev. Lett. **89**, 216802 (2002).

[25] S. A. Morton, G. D. Waddill, S. Kim, Ivan K. Schuller, S. A. Chambers and J. G. Tobin, Surf. Sci. Lett. **513**, L451 (2002).

[26] J. G. Tobin et al, MRS Symp. Proc. **524**, 185 (1998).

[27] E. Weschke, A. Höhr, G. Kaindl, S. L. Molodtsov, S. Danzenbächer, M. Richter, and C. Laubschat, Phys. Rev. B **58**, 3682 (1998).

[28] C. Bonnelle, R. C. Karnatak, and J. Sugar, Phys. Rev. A **9**, 1920 (1974).

[29] S. Pagliara, L. Sangaletti, C. Cepek, F. Bondino, R. Larciprete, and A. Goldoni. Phys. Rev. B **70**, 35420 (2004).

[30] S. R. Mishra, T. R. Cummins, G. D. Waddill, W. J. Gammon, G. van der Laan, K. W. Goodman, and J. G. Tobin, Phys. Rev. Lett. **81**, 1306 (1998).

[31] J. Kessler, *Polarized Electrons, 2nd Edition* (Springer-Verlag, Berlin, 1985).

[32] G. Crecelius, G. K. Wertheim, and D. N. E. Buchanan, Phys. Rev. B **18**, 6519 (1978).

[33] J. M. Esteva, R. C. Karnatak, J. C. Fuggle, and G. A. Sawatzky, Phys. Rev. Lett. **50**, 910 (1983).

[34] C. N. Berglung and W. E. Spicer, Phys. Rev. A **136**, 1030 (1964).

[35] J. Kirschner, R. Feder, and J. F. Wendelken, Phys. Rev. Lett. **47**, 614 (1981).

[36] G. D. Waddill, J. G. Tobin, X. Guo, and S. Y. Tong, Phys. Rev. B **50**, 6774 (1994).

[37] J. G. Tobin and F. O. Schumann, Surf. Sci. **478**, 211 (2001).

[38] E. Weschke, C. Laubschat, T. Simmons, M. Domke, O. Strebel, and G. Kaindl, Phys. Rev. B **44**, 8304 (1991).

[39] R. J. Elliott, Phys. Rev. **96**, 280 (1954).

[40] M. B. Zolfl, I. A. Nekrasov, Th. Pruschke, V. I. Anisimov, and J. Keller, Phys. Rev. Lett. **87**, 276403 (2001).

[41] K. Held, A. K. McMahan, and R. T. Scalettar, Phys. Rev. Lett. **87**, 276404 (2001).

[42] K. Haule, V. Oudovenko, S. Y. Savrasov, and G. Kotliar, Phys. Rev. Lett. **94**, 36401 (2005).

[43] R. G. Oswald and T. A. Callcott, Phys. Rev. B **4**, 4122 (1971).

[44] E. J. Cho, R. J. Jung, B. H. Choi, S. J. Oh, T. Iwasaki, A. Sekiyama, S. Imada, S. Suga, T. Muro, J. G. Park, and Y. S. Kwon, Phys. Rev. B **67**, 155107 (2003).

[45] O. Tjernberg, M. Finazzi, L. Duo, G. Ghiringhelli, P. Ohresser, and N. B. Brookes, Physica B **281**, 723 (2000).

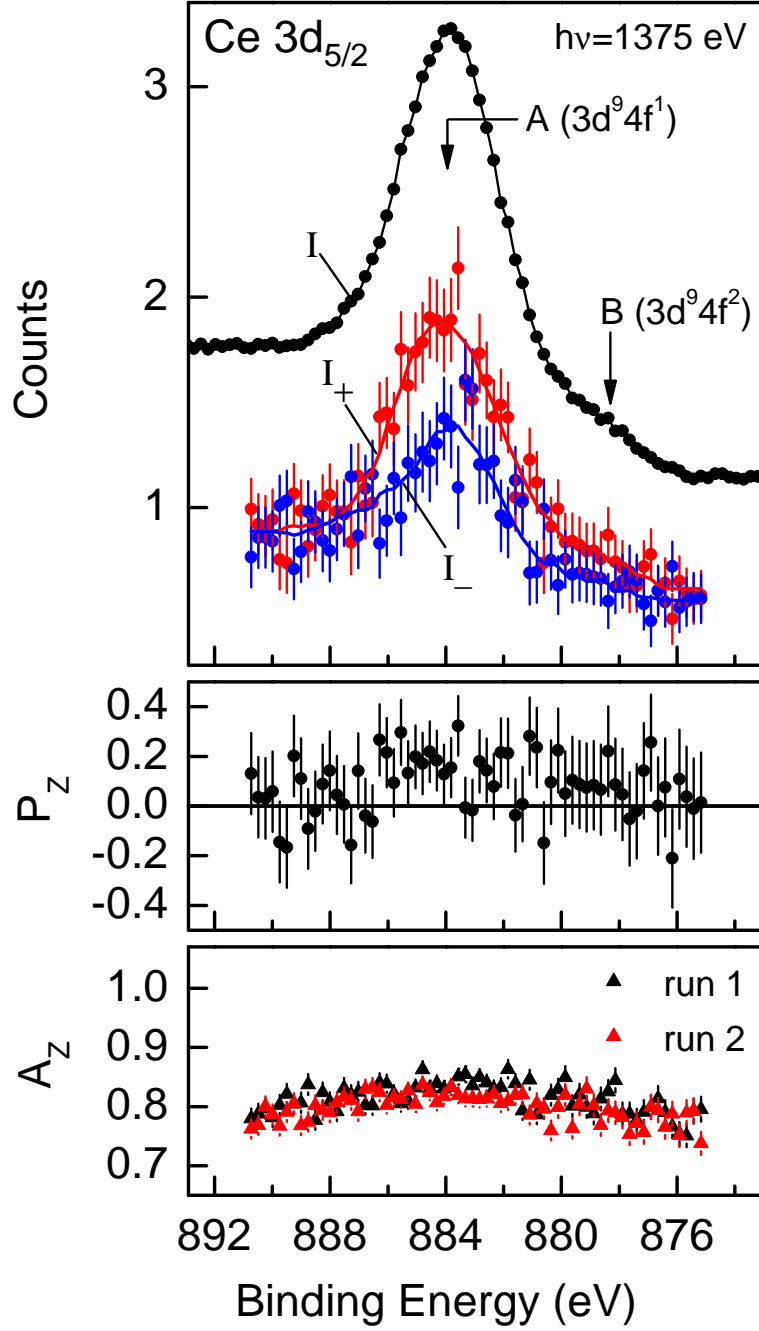[46] J. G. Tobin, S. A. Morton, B. W. Chung, S. W. Yu, G. D. Waddill, submitted to Physica B (2005).

13

FIG. 1: (Color) Top panel: Spin resolved $3d_{5/2}$ photoemission spectrum of Ce generated with circularly polarized light of hν=1375 eV. I is the spin integrated total intensity, and I_+ (red color) and I_- (blue color) are the two spin separated partial intensities. Solid lines on I_+ and I_- serve as a guide to the eyes. Middle panel: Electron spin polarization P_Z aligned with photon propagation direction determined by equation (3). The vertical error bars given in P_Z represent the single statistic uncertainties in the measured spin polarization. Bottom panel: Instrumental asymmetries A_Z determined by equation (4) for the two independent runs.
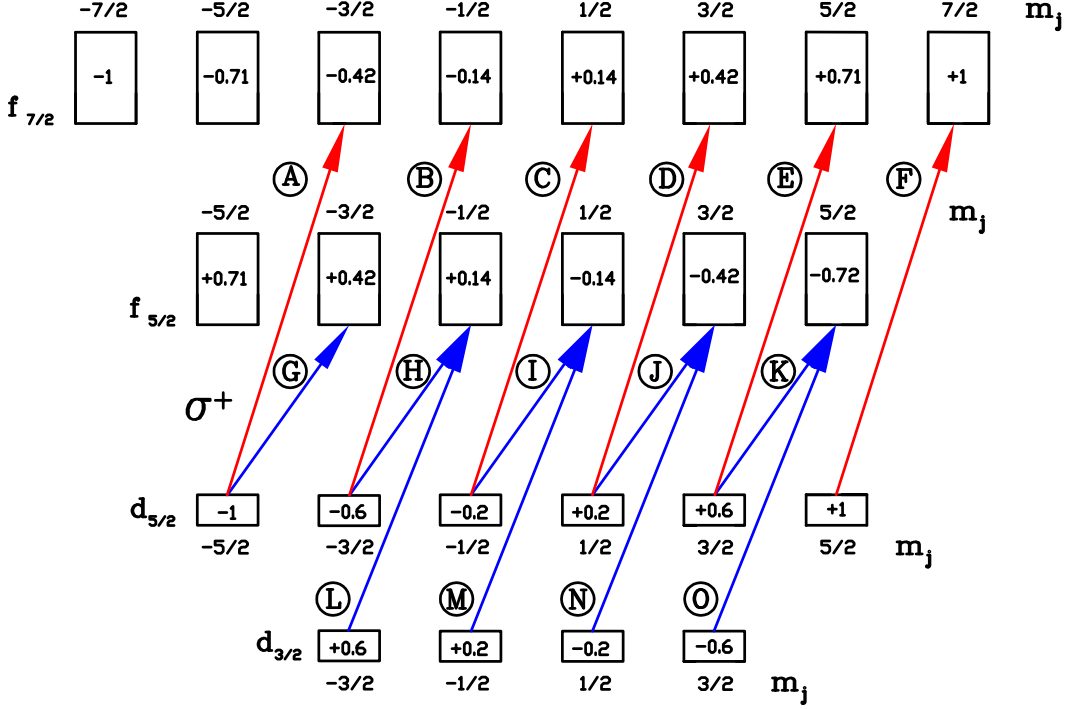
14

FIG. 2: (Color) Scheme of the photoexcitation $d \to f$ with σ^+. The arrows indicate the allowed transitions via relativistic dipole selection rules for σ^+ with the following transition probabilities normalized to transition G. A=5/2, B=15/2, C=30/2, D=50/2, E=75/2, F=105/2, G=1, H=8/5, I=9/5, J=8/5, K=1, L=49/10, M=147/10, N=147/5, O=49. Thereby, identical radial parts of the $d_{5/2}$- and $d_{3/2}$-wave functions and of the $f_{7/2}$- and $f_{5/2}$-wave functions are assumed. The arrows with red (blue) color represent transitions which give positive (negative) spin polarization of photoelectrons. The $d_{5/2} \to f_{5/2}$ transition gives a negative spin polarization, but it has 20 times weaker transition probability than that of the $d_{5/2} \to f_{7/2}$. Therefore, $d_{5/2} \to f$ ($f_{7/2}+f_{5/2}$) transition gives a net positive spin polarization of photoelectrons. Positive and negative numbers in the rectangles give the angle integrated spin polarization for given m_j using Clebsch-Gordan coefficients, e.g., for $m_j = -3/2$ of $d_{5/2}$, $|d_{5/2}, m_j = -3/2\rangle = \sqrt{1/5}Y_{2,-2}|\uparrow\rangle + \sqrt{4/5}Y_{2,-1}|\downarrow\rangle$ [9], therefore, -0.6 spin polarization. Energy differences are not to scale.
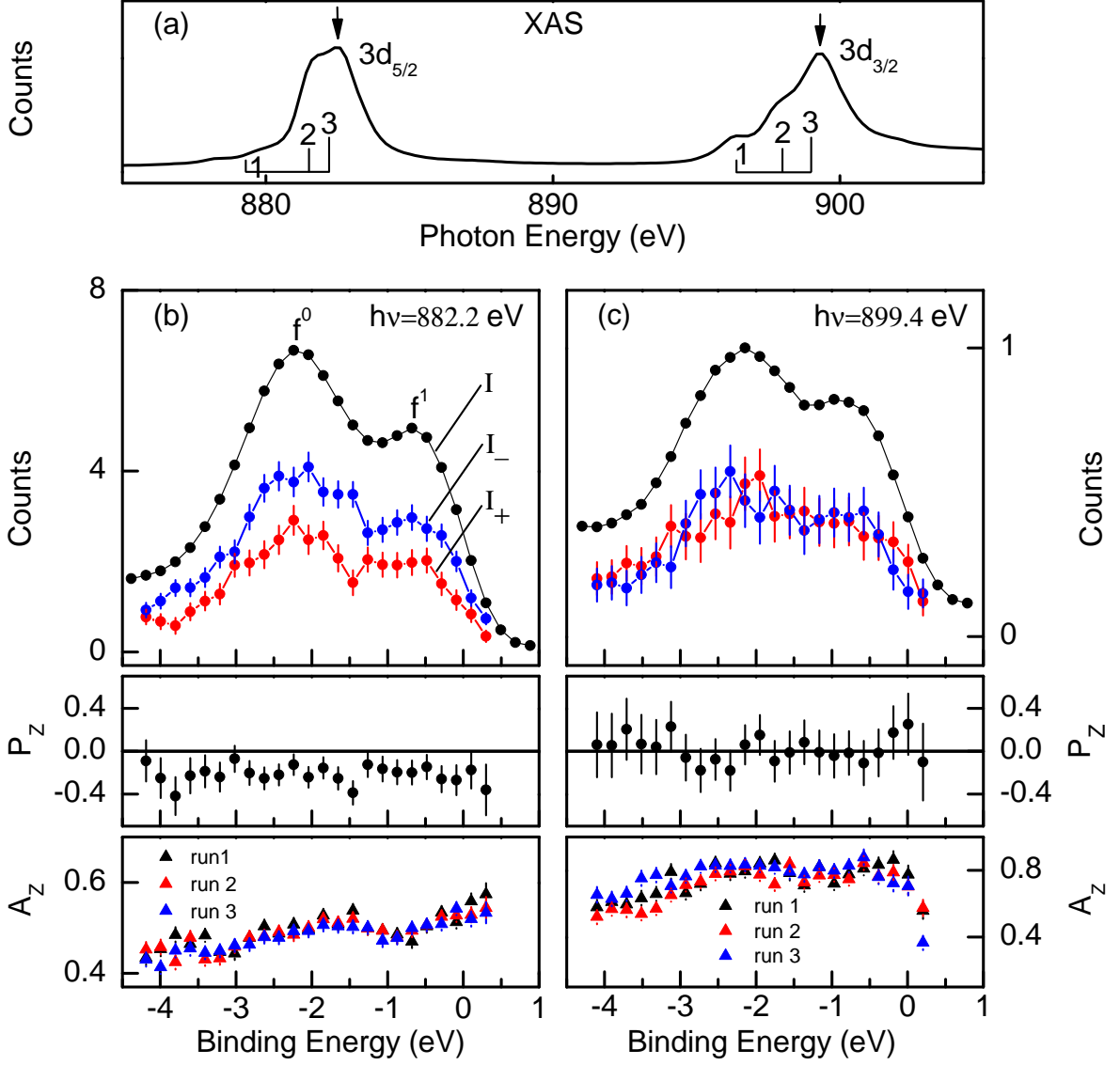
FIG. 3: (Color) (a) $3d \rightarrow 4f$ x-ray absorption spectroscopy (XAS) of Ce. Vertical lines with numbers indicate the observed three different multiplet states of the intermediate $3d^9 4f^2$ configuration from [28]. Arrows show the two photon energies used for spin resolved resonant photoemission measurements given in (b) and (c). (b) and (c) Spin resolved resonant photoemission spectra measured at $3d_{5/2} \rightarrow 4f$ at hν=882.2 eV and $3d_{3/2} \rightarrow 4f$ at hν=899.4 eV, respectively. I is the spin integrated total intensity, and I_+ (red color) and I_- (blue color) are the two spin separated partial intensities. For comparison, the total intensity of $3d_{5/2} \rightarrow 4f$ is normalized by that of $3d_{3/2} \rightarrow 4f$ at the position of f^0. The middle and the bottom panels of (b) and (c) represent electron spin polarization P_Z determined by equation (3) and instrumental asymmetries A_Z determined by equation (4) for the three independent runs, respectively.
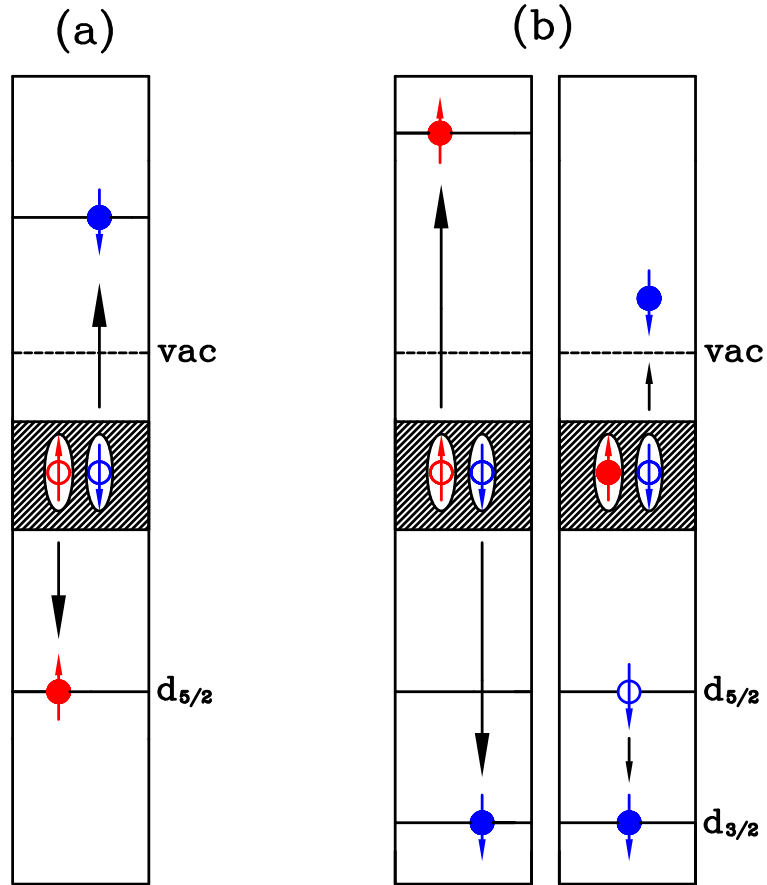
FIG. 4: (Color) (a) Sketch for a singlet coupling in a decay of spin polarized $3d_{5/2}$ core hole. (b) Sketch for a singlet coupling in a decay of spin polarized $3d_{3/2}$ core hole (left panel), with an additional Coster-Kronig transition (right panel). Here, the spin conserving Coster-Kronig process is assumed [10]. Energy difference is not to scale in (a) and (b).
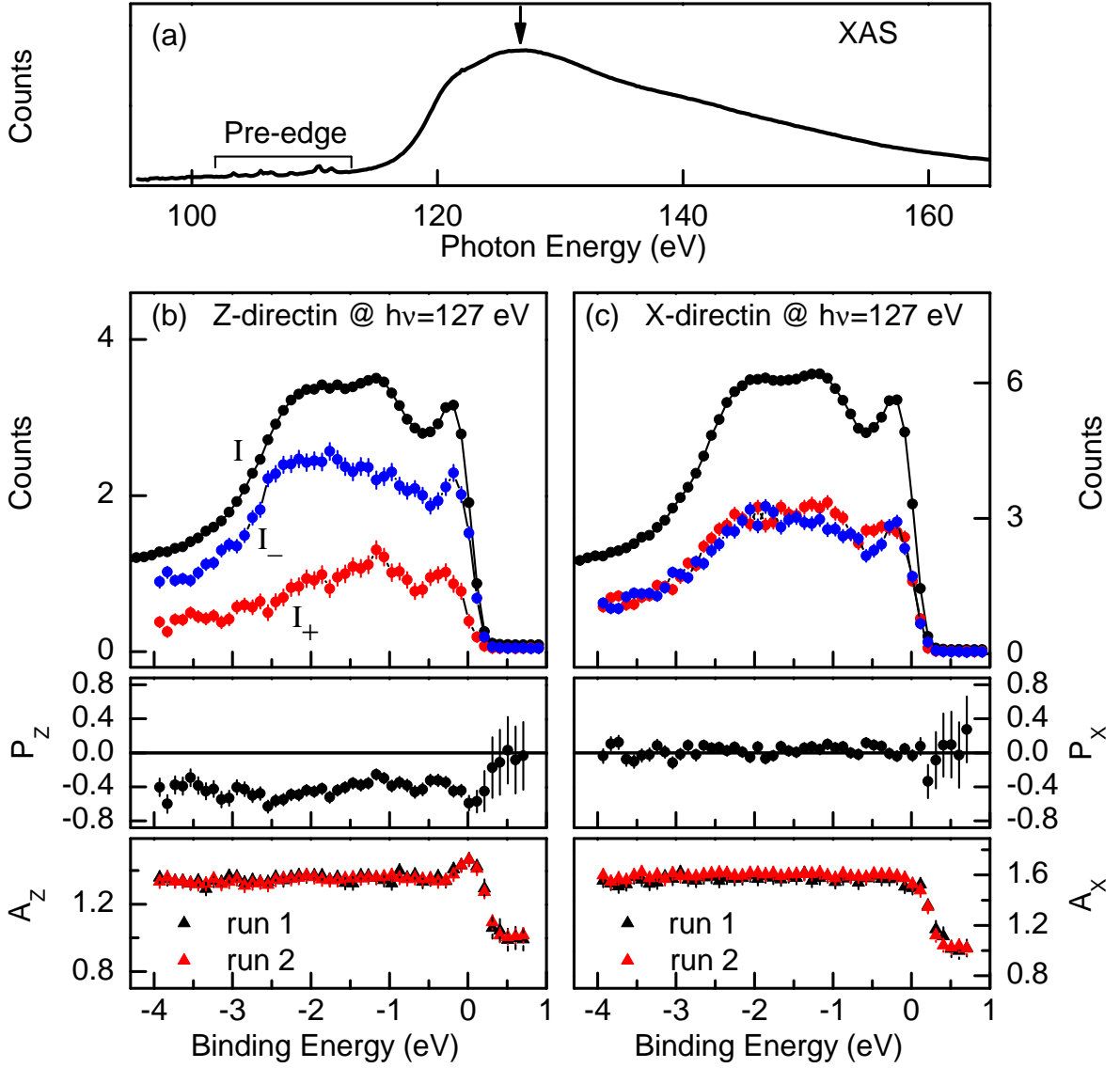
FIG. 5: (Color) (a) $4d \rightarrow 4f$ x-ray absorption spectroscopy (XAS) of Ce. Arrow shows a photon energy used for spin resolved resonant photoemission measurement given in (b) and(c). (b) Spin resolved resonant photoemission spectra measured at $4d \rightarrow 4f$ resonance along Z-direction (parallel to the photon propagation direction) at hν=127 eV. I is the spin integrated total intensity, and I_+ (red color) and I_- (blue color) are the two spin separated partial intensities. The middle and the bottom panels of (b) represent electron spin polarization P_Z determined by equation (3) and instrumental asymmetries A_Z determined by equation (4) for the two independent runs, respectively. (c) Spin resolved resonant photoemission spectra measured at $4d \rightarrow 4f$ resonance along X-direction (perpendicular to the photon propagation direction) at hν=127 eV. The middle and the bottom panels of (c) represent electron spin polarization P_X determined by equation (3) and instrumental asymmetries A_X determined by equation (4) for the two independent runs, respectively.

18